remote sensing

MDPI

Article

Characteristics of Aerosol Types in Beijing and the Associations with Air Pollution from 2004 to 2015

Yang Ou [1], Wenhui Zhao [2,3], Junqian Wang [4], Wenji Zhao [1,*] and Bo Zhang [5]

1 State Key Laboratory Incubation Base of Urban Environmental Processes and Digital Simulation, Ministry of Science and Technology, Capital Normal University, Beijing 100048, China; ouyangcnu@gmail.com
2 Beijing Municipal Environment Monitoring Center, Beijing 100048, China; wenhuidiandian@163.com
3 Beijing Key Laboratory of Atmospheric Particulate Matter Detection Technology, Beijing 100048, China
4 Department of Geography and Environmental Management, University of Waterloo, Waterloo, ON N2L 2R7, Canada; wajuqi@163.com
5 Information Center, Ministry of Environmental Protection, Beijing 100035, China; zhangbo@mep.gov.cn
* Correspondence: zhwenji1215@163.com; Tel.: +86-138-1070-7928

Received: 27 July 2017; Accepted: 28 August 2017; Published: 30 August 2017

Abstract: With the fast development of the economy and expansion, a large number of people have concentrated in Beijing over the past few decades, leading to the result that Beijing has become home to one of the most complex mixtures of aerosol types in the world. The various aerosol types play different roles in the determination of global climate change, visibility, and human health. However, to the best of our knowledge, research has rarely analyzed the correlation between aerosol types and air quality index (AQI) in Beijing (urban and suburban) over a long-term series of observations. Therefore, in this study, we aim to identify and discuss the different aerosol types and AQI in Beijing from 2004 to 2015. The aerosol types are classified into six categories: dust, mixed, highly-absorbing, moderately-absorbing, slightly-absorbing, and scattering by a multiple clustering method with the fine mode fraction (FMF) and single scattering albedo (SSA) data of retrievals from the global Aerosol Robotic Network (AERONET) sun photometer sites. The AQI levels: are good (0–50); moderate (51–100); unhealthy for sensitive groups (101–150); unhealthy (151–200); very unhealthy (201–300); and hazardous (>300). The results show that a significant FMF variability occurred among different seasons in Beijing, with maximum values present in spring and minimum values in winter. The SSA values exhibit variation, with small fluctuations from season to season. In the case of BJ station, the scattering aerosols are more frequent in summer (39%) and less in winter (1%), while the coarse particles (dust) are more frequent in spring (18%) and less in autumn (6%). In contrast, the absorbing aerosols (especially slightly-absorbing) are more frequent in summer (35%) and winter (15%). However, the mixed aerosol types are more frequent in spring (38%) and less in summer (8%). There is a similar seasonal variation in XH. In the past 12 years, the slightly-absorbing aerosol type in Beijing has increased by approximately 14%, which is believed to be due to the rapid development of industrial cities. In addition, comparing the urban and suburban regions, the slightly-absorbing aerosol type is the dominant aerosol type in both areas. Furthermore, to identify the dominant aerosol types which lead to air pollution, a related analysis was carried out by analyzing different aerosol types and the relationship between aerosol types and AQI. The results indicate that the air pollution was strongly correlated to slightly-absorbing aerosols, in which the percentage of slightly-absorbing aerosols was about 49% during the hazardous days in 2013–2015, and the correlation between AQI and aerosol types is also strong (R^2 = 0.76 and 0.97, in Beijing and Xianghe).

Keywords: aerosol optical properties; aerosol type; single scattering albedo (SSA); fine mode fraction (FMF); air quality index (AQI)

1. Introduction

Various aerosol types play significant roles in the determination of global climate change, air quality, and public health, which have been become important indicators in atmospheric environmental change detection [1–3]. Previous studies showed that aerosols affect the tendencies of the variations of air quality [4,5]. Additionally, different aerosol types originate from several sources with diverse physical and optical properties, and from various atmospheric impacts [6–10]. Each aerosol type has a different climatic effect due to their size and absorptive and scattering nature, such as dust particles having large sizes and sulfate aerosols having a scattering nature, whereas nitrate particles with small sizes have absorbing tendencies [7,8,11–16]. Consequently, long-term measurements of aerosol optical properties and aerosol types at a large scale are necessary to interpret the aerosol climatic effect [17,18].

Beijing is influenced by the duality of the natural climate and anthropogenic activities due to its dense population and high pollution emissions, resulting in many severe environmental problems [19–22]. Heavy air pollution hazes largely caused by high aerosol loading have frequently occurred in Beijing [23–25]. Meanwhile, the heavy air pollution is reflected in an especially sharp increase in respiratory diseases [19,20,26]. Therefore, it is essential to understand the impact of aerosol types on air quality through the study of aerosol optical properties for long periods in Beijing [18,20,27,28].

Numerous previous studies provide abundant information to the discussion of the seasonal aerosol types by using ground-based and satellite-based measurements in Beijing [24,27,29–37]. In spring, the majority of heavy aerosol pollution is associated with dust. Dust storms occur annually during the spring season, and large quantities of dust are occasionally transported to Beijing from the deserts in Western China [24,33]. By contrast, in summer and autumn, the contribution of photochemical secondary aerosol formation and biomass burning are high. In the case of a severe pollution event in June in Beijing, it has been shown that burning plays a significant role in exacerbating the air quality [38]. Meanwhile, the aerosol scattering coefficient increased significantly and showed a different spatial distribution under different conditions during haze events [39]. Thus, biomass burning in the Beijing region is an important pollution factor that cannot be neglected in the summer and autumn [18,37,40,41]. Moreover, in winter, the occurrence of haze episodes is more frequent and severe, due to the increased pollutant emissions from coal combustion for house heating and unfavorable meteorological conditions [19,37,42]. Li et al. [28] investigated two haze events in Beijing which occurred in winter and retrieved aerosol chemical composition fractions.

Although many studies have been made on the seasonal aerosol types in the past two decades in Beijing, only a few studies have distinguished the various aerosol types over a long-term. For example, Yan et al. [39] found that four general aerosol types (polluted, relatively polluted, clean, and relatively clean) are associated with different sources and emission mechanisms by the hygroscopic growth function of the aerosol scattering coefficient, f(RH). However, Li et al. [43] identified sulfate, nitrate and dust as the three aerosol types based on the differences in visibility and relative humidity during the two types of haze episodes. Eck et al. [44] distinguish the fine mode pollution aerosols, coarse mode aerosols and mixtures of fine and coarse aerosols, as the three aerosol types as determined by the FMF, absorption Ångström exponent (AAE) and aerosol absorption optical depth (AAOD). Wang et al. [45] studied the seasonal changes in the main types (dust sulfate aerosols; fine-mode aerosols; mixed aerosols) of aerosol over northern China by using the Ångström exponent (AE) and AOD. Meanwhile, Eck et al. [44] and Wang et al. [45] evaluate the changes of aerosol optical properties in coarse/fine modes by discussing the aerosol types. Yu et al. [46] presented the dominance of fine particles, which are more scattering particles, by studying the characteristics of aerosol optical properties in spring during 2001–2014 over urban Beijing. Wang et al. [47] pointed out that nitrates and sulfates were the major aerosol types on haze days in Beijing, which is consistent with the conclusion draw by Li [28]. Li et al. [48] and Chen et al. [49] analyzed the aerosol properties variations over a long-term via AERONET ground-based observations in Beijing and Xianghe stations. Meanwhile, a summary of aerosol optical properties of major aerosol types has been recorded in urban and suburban environments [48,49].

From our literature review, we found that most of the abovementioned studies were limited to urban study sites [39,43,44]. There are only a few studies focusing on the distinction of aerosol types over urban and suburban sites in Beijing [28,49]. Particularly, the time span of previous studies were mostly for short-term characteristics of aerosols, while fewer studies focused on the long-term (over 10 years) characteristics in aerosol optical properties [23,49]; particularly, the correlation between aerosol types and air quality over Beijing remain a knowledge gap in the existing literature. Therefore, the objectives of this study are three-fold: (1) categorize atmospheric aerosols into six abovementioned types according to the optical properties, and the dominant aerosol type in different seasons and stations was identified; (2) investigate the change of the aerosol type over a long-term period (2004–2015); and (3) use the air quality index (AQI) to analyze the relationship between aerosol types and air quality over urban and suburban Beijing.

2. Materials and Methods

2.1. Study Sites

Beijing is located at 39.92°N, 116.46°E, which is on the North China Plain. It covers an area of 16,410 km^2, and its terrain is characterized as mountainous in the northwest and plains in the southeast (Figure 1). Beijing shows the typical characteristics of a temperate-zone land climate with four distinctive seasons. The annual precipitation is approximately 640 mm, which mainly occurs during summer [50]. As a diversified and fast-developing city, Beijing has a dense population and serious atmospheric pollution. The vast amount of atmospheric pollutants primarily originates from major pollution sources, such as air discharges from vehicles and coal burning. In this study, two ground-based observation stations in Beijing are used (Beijing (BJ) and Xianghe (XH)) (Table 1). These stations represent different locations and land cover, i.e. urban and suburban regions (Figure 1). Beijing can be divided into two districts geographically: urban and suburban. The population in urban is larger than suburban. The urban area accounts for 8.44% of the total area in Beijing, while the population accounts for 62.6% of the total population, and the population density is up to 5882 people/km^2, which is higher than the average population density of Beijing (848 people/km^2). The suburban area accounts for 91.85% of the total area in Beijing. The suburban population accounts for 37.32% of the total population, and the population density is 346 people/km^2, which is less than half of the average population density of Beijing [51].

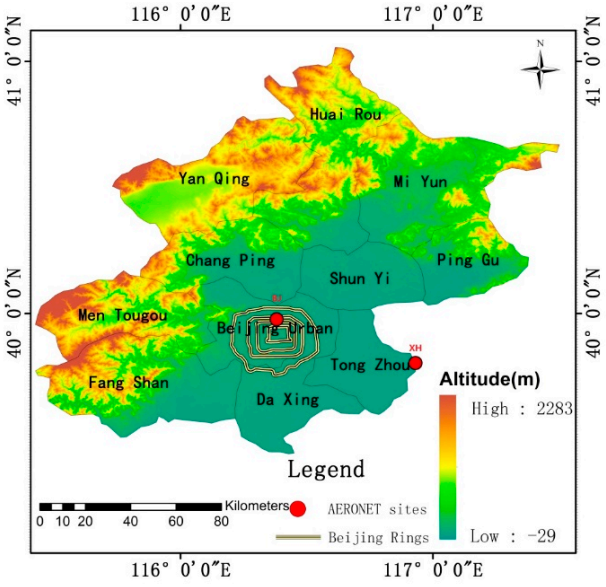

Figure 1. AERONET sites in Beijing.

Table 1. AERONET sites.

Sites	Lng E/Lat N	Observation Time	Sample Number
Beijing (Urban)	116.381/39.977	September 2004–December 2015	2336
Xianghe (Suburban)	116.962/39.754	September 2004–December 2015	2554

2.2. AERONET Data

AERONET is a ground observation network comprised of a group of ground-based remote-sensing aerosol sites established by NASA to detect the global atmospheric aerosol (http://aeronet.gsfc.nasa.gov) [52]. It covers more than 800 sites in the world, but only few of the AERONET stations in China perform long-term measurements. There are four sites in Beijing [53]. The program provides a long-term, continuous, and readily-accessible public database of optical, microphysical, and radiative aerosol properties for aerosol research [7,13,54–58]. The products retrieved from AERONET include aerosol optical depth, Ångström exponent, aerosol size distribution, single scattering albedo (SSA), fine mode fraction (FMF), refractive indices and asymmetry factor, which use standardized instruments, calibration, processing, and distribution, verifying the accuracy of the satellite remote sensing inversion results, and are used as ground observation values by global researchers [3,14,59–61]. The central wavelengths of the French-made Cimel 318 radiometer are 340 nm, 380 nm, 440 nm, 670 nm, 870 nm, 940 nm, 1020 nm and 1640 nm. The accuracy is 0.01–0.02 in the absence of unscreened clouds for validating satellite-derived Aerosol Optical Depth (AOD) values in the visible and near-infrared ranges [8]. Meanwhile, AERONET provides AOD, SSA, FMF, aerosol size distribution, refractive indices, and other products, which can represent the absorptivity, fine particle ratio, aerosol volume distribution, scattering direction and other aerosol optical and physical properties [59]. The products provided by AERONET at a temporal resolution every 15 min are categorized in three levels: Level 1.0 (unscreened), Level 1.5 (cloud-screened), and Level 2.0 (cloud-screened and quality-assured).

In this study, the product (SSA and FMF) of Level 1.5 was selected, which was acquired from two ground-based observation stations (BJ and XH). The level 1.5 data enable cloud screening and additional quality control, including quality checks, stability criterion check and standard deviation check, and have continuous long-term observations for more than ten years [62]. Although the level 2.0 data provide more accurate products than level 1.5, they provide significantly fewer data points. Therefore, in long-term observations, the level 1.5 products of BJ and XH stations were chosen for analyzing the optical properties in urban and suburban regions owing to the long-term coverage.

2.3. Aerosol Classification Methods

Aerosols can be classified into six major types because the optical properties of aerosols show obvious distinctions [15]. In this study, two important microphysical properties (SSA and FMF) that which represent the radiation absorptivity and consider the size of aerosol are used for classification [9]. FMF is defined as the ratio of the AOD of the fine particles to the total AOD, which is used to represent the contribution of fine particles (Equations (1) and (2)). Therefore, FMF at 550 nm is used to determine the dominant size mode. SSA is one of the most significant optical parameters for climate change, which is defined as the ratio of the scattering coefficient to the extinction coefficient of the total aerosol column (Equation (3)).

$$\mathrm{FMF} = \tau_m / (\tau_m + \tau_c) \tag{1}$$

$$\mathrm{AOD} = \int_0^t k(\lambda, h) dh \tag{2}$$

$$\mathrm{SSA} = \delta_{sc} / (\delta_{sc} + \delta_{ab}) \tag{3}$$

where τ_m is the fine AOD; τ_c is the coarse AOD; t is the vertical atmospheric depth; $k(\lambda, h)$ is the extinction coefficient; h is the per unit distance; δ_{sc} is the total scattering coefficient; and δ_{ab} is the total absorbing coefficient.

Therefore, the SSA at 440 nm is used to distinguish absorbing from non-absorbing aerosols. Subsequently, to determine the aerosol types by using the classification algorithm with FMF and SSA from AERONET, the threshold for FMF and SSA have been determined as follows: The FMF >0.6 means that the fine particles contribute more to AOD and the FMF <0.4 means that the coarse particles contribute more to AOD. The mixed aerosol is considered between 0.4 and 0.6, which is a mixture of coarse and fine particle aerosols. The contribution of fine and coarse particle to total AOD is almost equal. The SSA is used to distinguish absorbing and scattering aerosols, while 0.95 is the threshold [9,63]. The absorbing aerosols are further divided into highly-absorbing, moderately-absorbing and slightly-absorbing types by SSAs (Figure 2). Thus, the combination of SSA and FMF can provide the particle size and radiation absorptivity. The classification method is shown in Figure 2 [9]. Consequently, these aerosol types are dust, mixed, highly-absorbing, moderately-absorbing, slightly-absorbing, and scattering. In addition, the indeterminate type is less than 2%, which is not involved in our discussion.

Figure 2. The flowchart of the aerosol classification algorithm created by using FMF and SSA from AERONET: N (Dust) = 382; N (mixed) = 1061; N (highly-absorbing) = 530; N (moderately-absorbing) = 995; N (slightly-absorbing) = 1246; and N (scattering) = 628 (Ns are the totals for both BJ and XH sites).

3. Results and Discussion

3.1. Optical Characteristics of Different Aerosol Types

To analyze the annual and seasonal optical properties of various aerosol types, the change of annual and seasonal mean FMF and SSA has been discussed.

3.1.1. Seasonal Variation of Different Aerosol Optical Properties

In this study, the season is simply divided into four periods: winter (December to February), spring (March to May), summer (June to August), and autumn (September to November). With weather conditions and human activity factors varying during different seasons, the optical properties of aerosol particles also vary with the seasons. The average values of FMF and SSA were calculated by the data over a 12-year period in each season. Figure 3 illustrates seasonal changes of FMF and SSA, which were collected for BJ and XH stations from 2004 to 2015. From the view of the FMF, the dominant fine particles are significant in summer and autumn, as compared to spring and winter, where the reverse is the case. Similarly, the SSA has a similar seasonal variation with less fluctuation. In spring, FMF was at the lowest point (0.56 in BJ and 0.62 in XH), because of frequent dust storms in the north. However, during the summer period the FMF and SSA increase dramatically to 0.80 and 0.93 in BJ, respectively, because the improvement of oxygen conversion of particles will rise greatly in summer with the higher temperature which is a possibility that cannot be excluded. Conversely, the values of autumn declined, and significantly degraded to 0.67 and 0.89 possibly due to rainfall. A similar variation during the winter period exists, with the FMF and SSA degrading to 0.61 and 0.87 in BJ, respectively. There is a similar seasonal variation in XH.

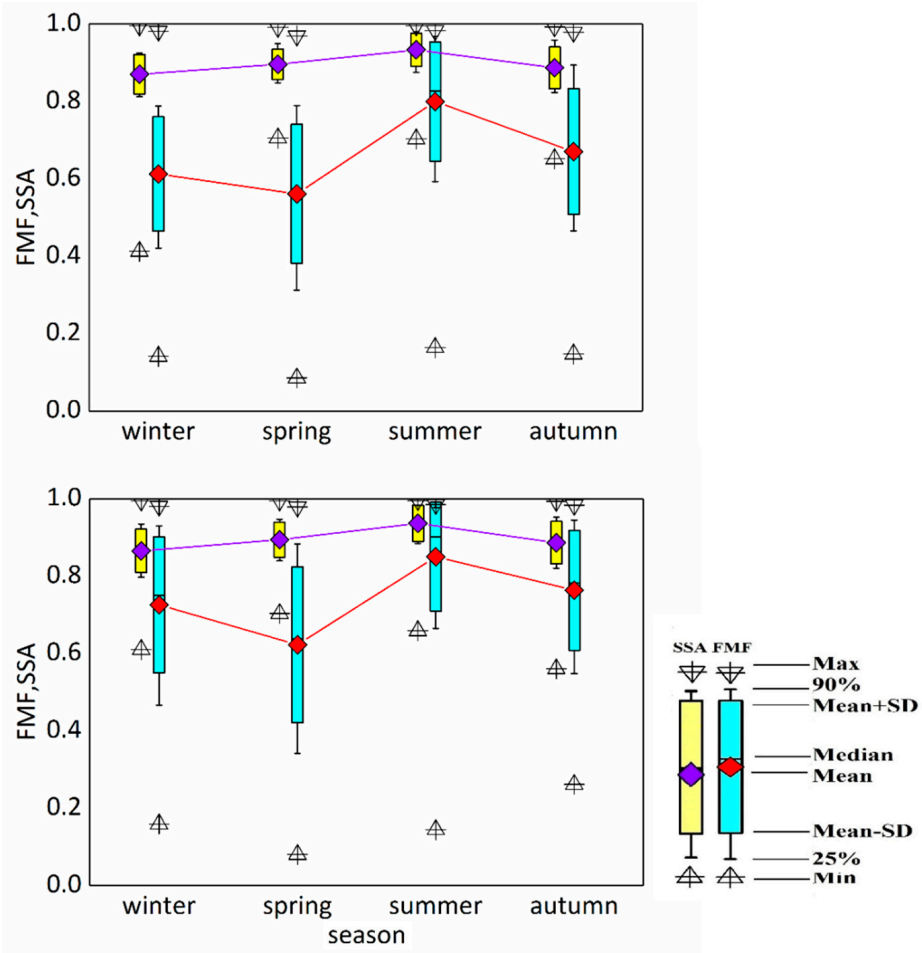

Figure 3. Seasonal variation of the aerosol types in BJ and XH.

3.1.2. Annual Variation of Different Aerosol Optical Properties

Figure 4 compares the change of two different kinds of optical properties, namely, FMF and SSA during a 12-year period from 2004 to 2015 in Beijing. The annual averages of FMF and SSA were calculated using 12 years of data. With respect to the fraction of FMF, it dropped by 0.04

from 2004 to 2006, bottoming at 0.60, and then there was a slight increase from 2012 to 2015 in BJ. In contrast, the bottom of XH is 0.69 in 2006 and then there was an increase until 2009. Meanwhile, there was an inconspicuous decrease in the SSA over the period. Moreover, it witnessed inconsiderable fluctuations from 2009 (0.91) to 2015 (0.91) in BJ, but there was an increase from 2009 (0.71) to 2015 (0.79) in XH. To sum up, FMF decreased during 2004–2006 and then followed with slight increase, while the fraction of SSA was stable. The pollution of fine particles was very serious because of the anthropogenic pollution, such as industrial emissions, automobile exhaust, and construction dust.

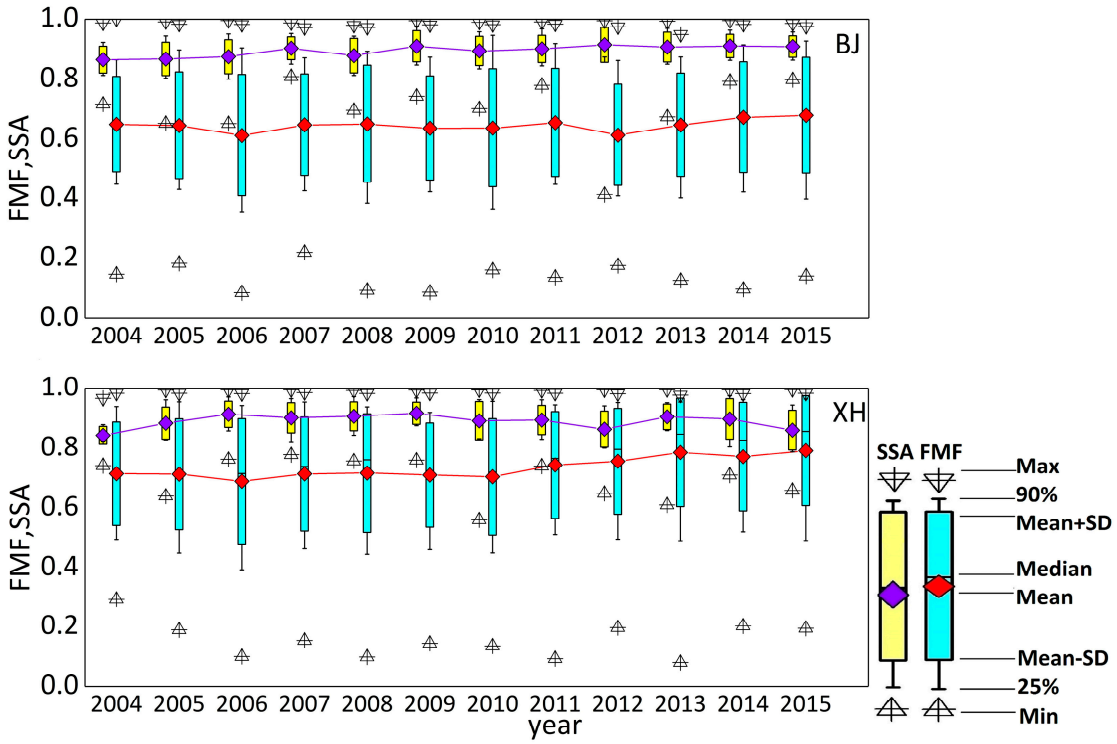

Figure 4. Annual average variation characteristics of the optical properties in BJ and XH.

3.1.3. Optical Properties of Different Aerosol Types

In terms of the FMF of different types (Figure 5), the FMF of dust is small due to the large particle radius (the mean of FMF is 0.30), and the mean FMF of mixed types is 0.52, which is significantly higher than that of dust. The FMF of scattering was the highest, at 0.88. The FMF values of the three absorbing types were similar, with means of 0.80, 0.75, and 0.73. In general, the fine particles were produced by human activities which led to high values of FMF, relatively, and the characteristics of the composition and physicochemistry of atmospheric particles have differences in spatial distribution [26]. In contrast, compared with the SSA of different types (Figure 5), the value of the scattering type is the highest (at 0.97); the second are dust and mixed types; with average values of 0.87 and 0.88. It is worth noting that the scattering properties of the mixed type are related to the mineral composition [64]. The SSA of slightly-absorbing, moderately-absorbing, and highly-absorbing types increases gradually, which are 0.92, 0.88 and 0.81, respectively. Moreover, the amplitude between the maximum and minimum is 0.16 (about 16%).

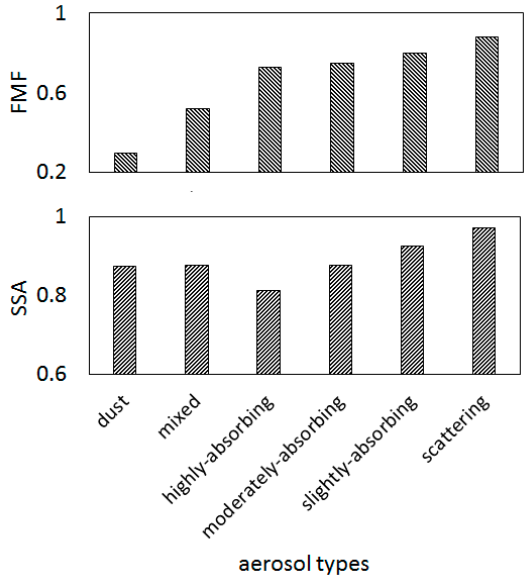

Figure 5. Average optical properties of different aerosol types (FMF and SSA).

3.2. Comparison of Aerosol Types in Urban and Suburban Regions

3.2.1. Seasonal Variation of Different Aerosol Types in BJ and XH

In terms of weather conditions in different seasons, the monthly and seasonal variations of aerosol types between urban and suburban regions in Beijing have been calculated. In comparison with the percentage of different aerosol types, the mixed type is dominant in spring (March, April, and May), but the percentage in BJ is nearly double that in XH. The slightly-absorbing remains the highest throughout all of the seasons in both stations, especially in summer (Figure 6). Moreover, the variation of slight-absorbing shows a decrease from about 35% in summer (June, July, and August,) to around 15% in winter (December, February, and January) in BJ. Similarly, the scattering degrades from 39% in summer (June, July, and August,) to 1% in winter (December, February, and January) in BJ. It may be related to the meteorological conditions of summer. The surface ground received more energy to complete the atmospheric turbulence because of the long duration of sunshine. It creates the advantaged conditions for pollutant dispersion and secondary aerosol generation. In addition, the southern winds are prevailing in summer. Hence, the regional transport may contribute more to aerosol pollution in Beijing. In contrast, the moderately-absorbing and highly-absorbing types are significant in winter with approximately 26% and 16%, then drop to less than 13% and 3% in the summer in BJ. There is a similar seasonal variation in XH.

To summarize the variations of overall aerosol types, the monthly percentage of slightly-absorbing aerosols in both stations were higher than other aerosol types in recent years (12-year period), and the monthly percentage of dust is minimal. As an illustration, agricultural crop residue burning mostly occurred in the period of May to September in North China [32]. The aerosols that were released from the surrounding farmland increased the slightly-absorbing type in summer [40]. Furthermore, high humidity during monsoons leads to more moisture absorbing aerosol and contributes to air pollution [65]. Fine particles will increase in the case of high temperature and humidity [45]. Therefore, the average temperature and average humidity both seem to be other important factors that should be considered. It can be concluded that fine particle aerosols were the dominant type during the summer and autumn.

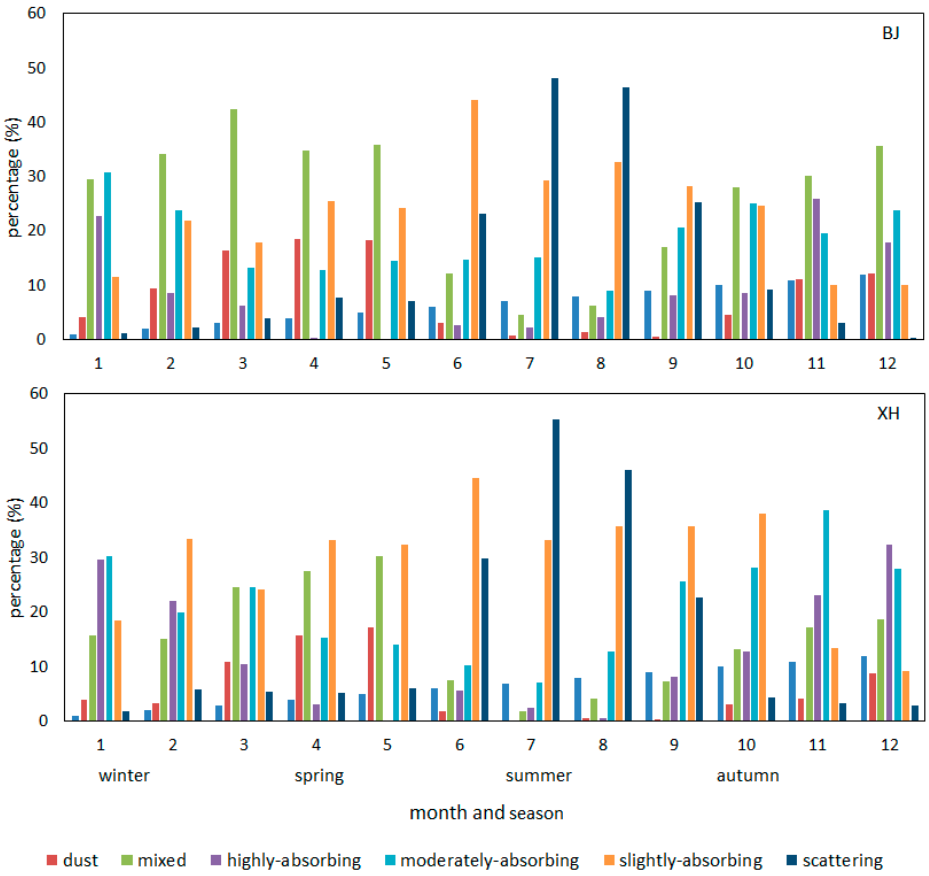

Figure 6. Monthly and seasonal percentage of aerosol types at different stations in BJ and XH (N = 2336 and N = 2554, respectively).

3.2.2. Average Proportion of Aerosol Types over 12 Years in BJ and XH

Figure 7 shows a similar distribution of six main aerosol types by comparing the distributions of the annual mean aerosol types between BJ and XH stations from 2004 to 2015. At the BJ station, the slightly-absorbing aerosol type is 22%, which was possibly caused by too much industrial emission and vehicle exhaust. The other absorbing aerosol types (highly- and moderately-absorbing types) annually constitute 9% and 19%, respectively. A further 28% of aerosol types is mixed, which is due to overly-complex air pollution. Dust accounts for only 10%, collectively. In addition, the scattering aerosols contributed to 12% of the aerosol types. In the case of XH station, the percentage of aerosol types in the suburban region is similar with that of the urban region. The proportion of slightly-absorbing aerosols is also the highest, and it is more than the urban region, by around 6%. A slight difference of the other aerosol types between urban and suburban regions also exists (dust, 4%; moderately-absorbing, 3%; highly-absorbing, 4%; and scattering, 2%). The apparent gap for the mixed types between stations is especially large at 11%.

To summarize, the slightly-absorbing aerosol type is the main type in the BJ and XH stations, which were mainly caused by heating in winter, automobile exhaust, aggravation of the incomplete burning of coal, and other factors. Based on previous research, it is known that particles of coal have the high absorbing ability and the stable meteorological conditions are beneficial for coal particles to accumulate. Additionally, as shown in the Figure 7, the absorbing aerosol types (highly-absorbing, moderately-absorbing, and slightly-absorbing) account for 50% in the urban region, and these account for 63% in the suburban region. This result is consistent with the conclusion drawn by Li et al. [28] that the dominant aerosol types are absorbers, and the weak absorption aerosol type mainly occurs in the summer.

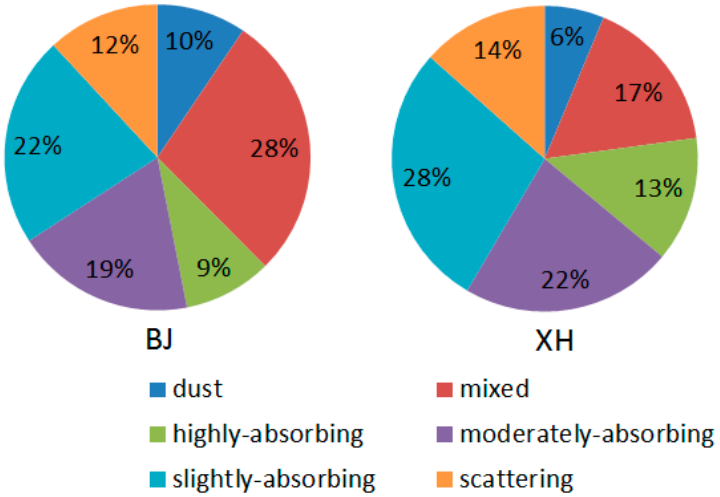

Figure 7. Distribution of different aerosol types at BJ and XH sites.

3.2.3. Annual Variation of Different Aerosol Types in BJ and XH

Figure 8 shows the annual percentage of the aerosol types in BJ and XH from 2004 to 2015. In the case of the BJ urban station, the mixed and slightly-absorbing aerosols are the dominant aerosol types throughout this period, with the highest points at 40% and 33% (Figure 8) in 2012 and 2014, respectively. The mixed aerosols overtook the slightly-absorbing type in 2004, becoming the highest since then. However, the gap between mixed and slightly-absorbing types narrowed considerably in 2007, and the gap increased gradually until 2013.

Despite the scattering aerosols having some fluctuation, the highest value between 2004 and 2015 occurred in 2013 with the highest point at 21% since 2004. Dust, and moderately-absorbing and highly-absorbing aerosols are similar, remaining stable over the period with slight fluctuation (under 30%). Conversely, the slightly-absorbing type is still higher than the others from 2005 at the XH station and the period 2004–2015 witnessed a decrease of the mixed type from 21% to 9%, whereas the scattering type fell back to 10% from 2008 to 2015 after initially rising. Overall, the slightly-absorbing types are still the dominant aerosol types in the period of 12 years, which is relatively significant compared with the remaining types (it increased by approximately 14%).

Previous research has demonstrated that absorbing aerosols (including black carbon) play an important role in urban environments [21]. Therefore, we hypothesize that the reason for the annual variation of aerosol types in Beijing is related to black carbon emissions. Chen et al. [66] found that the black carbon emission variations fluctuated from 2005 to 2012 (increasing from 2005 to 2007, and then decreasing in 2008). After 2008, BC emissions rose again in 2009, and then declined slightly in 2012 because of air pollution control plans for the 2008 Olympic Games and natural gas was widely used instead of coal in urban households [67]. Through the results of the aerosol type classification in this study, the variations of black carbon emissions and the slight-absorbing aerosol type are consistent, which probably indicates that black carbon is a component of the slight-absorbing aerosol type. Future work could explore how the black carbon emissions may affect the variation of aerosol types in Beijing.

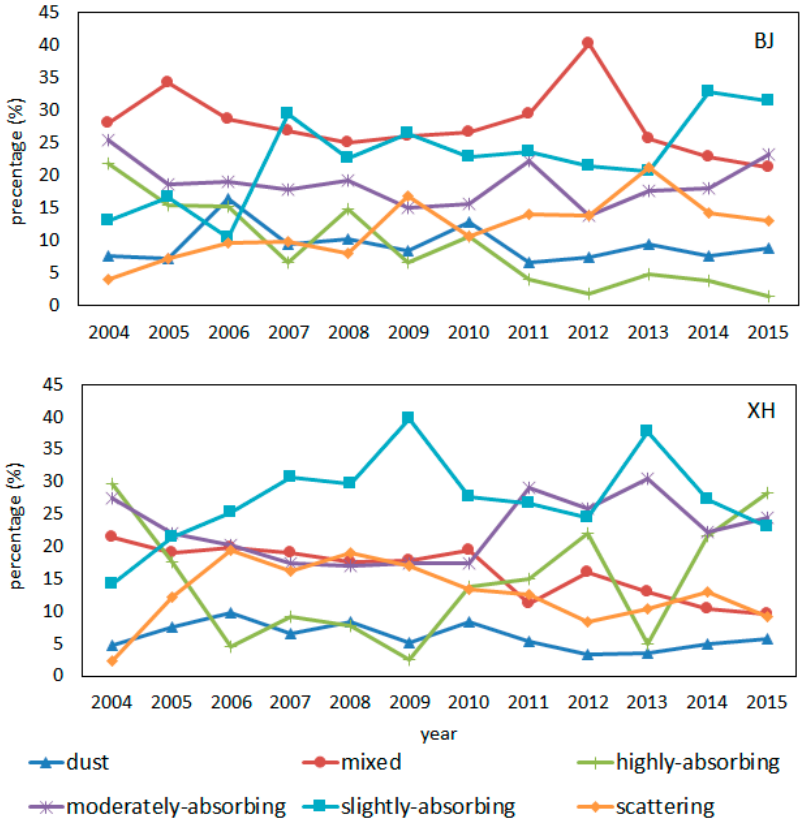

Figure 8. A time series of the aerosol types in BJ and XH stations in the past 12 years.

3.3. Correlation between AQI and Aerosol Types

The relationship between air quality and aerosol types for the BJ and XH stations over a period of three years (2013–2015) was analyzed, based on the surface monitoring data air quality index (AQI) in Beijing. The surface monitoring data (AQI) were downloaded from the Beijing Municipal Environmental Monitoring Center service system (http://www.bjmemc.com.cn/). China's AQI is a sophisticated and widely used index to communicate the health risk of ambient concentrations [68]. Since 1 January 2013, the Beijing Municipal Environmental Protection Bureau (BMEPB) published the daily AQI instead of the API (Air Pollution Index). This is typically a numerical scale which includes indices for O_3, PM, CO, SO_2 and NO_2 and it is intended to convey the health impact of air pollution. The range of AQI is from 0 to 300+, which includes good (0–50); moderate (51–100); unhealthy for sensitive groups (101–150); unhealthy (151–200); very unhealthy (201–300); and hazardous (>300) levels.

3.3.1. The Incidence of each Aerosol Type at Specific AQI

The recorded days of the aerosol types in 2013–2015 are shown in Figure 9. The aerosol type shown in Figure 9 was the dominant one on each day. In this study, AQI and aerosol types were matched by time, and the portions in bold represent the dominant aerosol types in the various AQI level (Tables 2 and 3). Moreover, the number of days for each aerosol type and the proportion of major aerosol types were calculated by using AQI as the standard pollution levels. Tables 2 and 3 are the days of the different aerosol types at specific air quality levels. The unhealthy for sensitive groups level is the most populous among the six air quality levels. It was dominant with 315 days in the two sites over three years. The moderate level is the second with 293 days, followed by good, unhealthy, very unhealthy, and hazardous. The hazardous day level was the least populous (66 days), but it hurts human health seriously, and can cause many respiratory diseases. The primary aerosol type in the hazardous category is the slightly-absorbing types (approximately 49%).

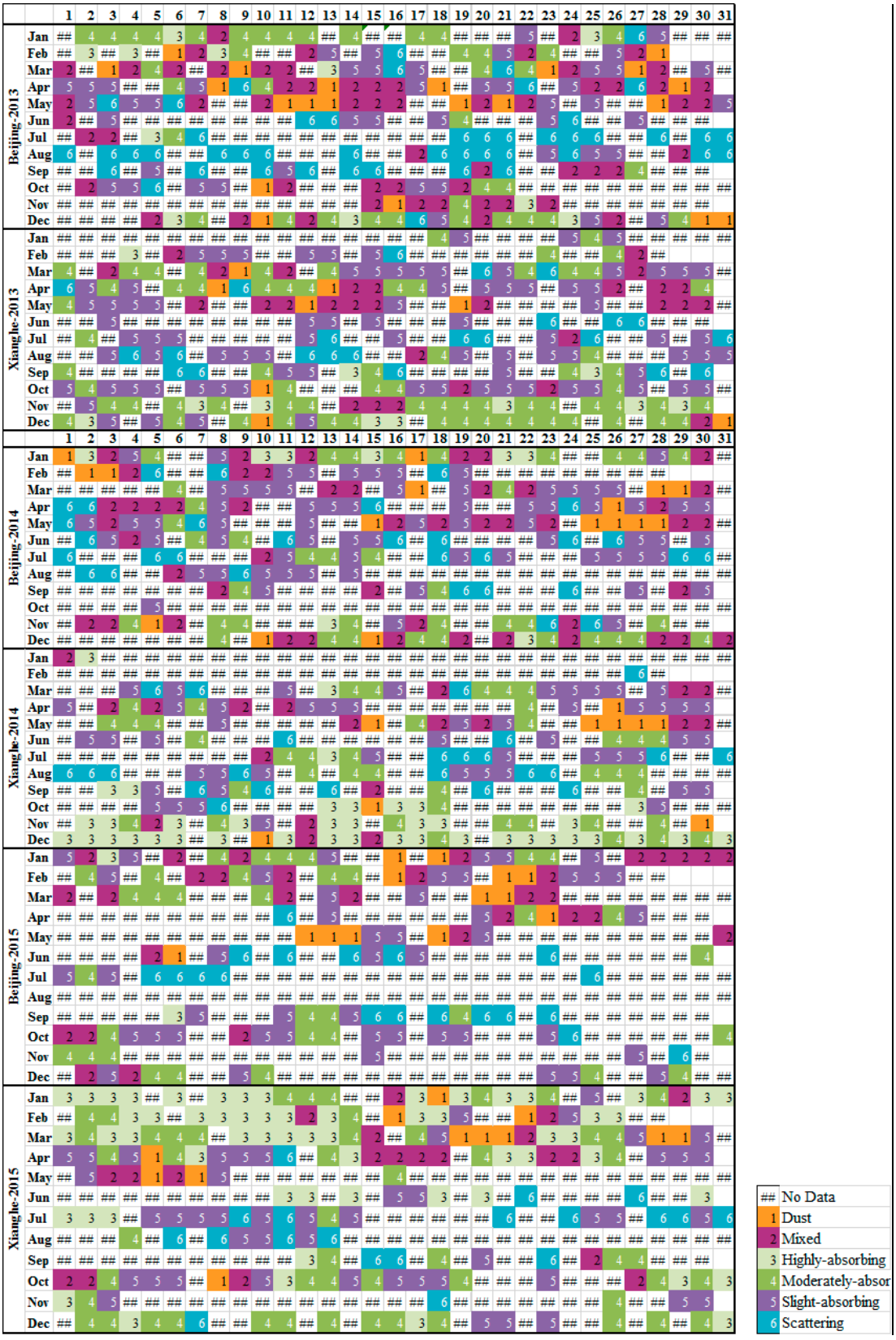

Figure 9. The recorded days of aerosol types in 2013–2015.

Table 2. The percentage of aerosol types in different air quality levels (2013–2015) by the range groups of the daily average of AQI at the BJ site. N = 575 (the values in bold are the days of the dominant aerosol types).

AQI	Dust	Mixed	Highly-Absorbing	Moderately-Absorbing	Slightly-Absorbing	Scattering	Total	Dominant Aerosol Type %
Good (0–50)	6	**52**	5	25	21	14	123	42
Moderate (51–100)	11	35	2	23	**40**	12	123	33
Unhealthy for Sensitive Groups (101–150)	18	**36**	9	30	33	31	157	23
Unhealthy (151–200)	12	8	2	13	**29**	28	92	31
Very Unhealthy (201–300)	2	2	2	15	**24**	6	51	47
Hazardous (>300)	1	3	1	5	**14**	5	29	48
total	50	136	21	111	**161**	96	575	28

Table 3. The percentage of aerosol types in different air quality level (2013–2015) by the range groups of the daily average of AQI at the XH site. N = 615 (the values in bold are the days of the dominant aerosol types).

AQI	Dust	Mixed	Highly-Absorbing	Moderately-Absorbing	Slightly-Absorbing	Scattering	Total	Dominant Aerosol Type %
Good (0–50)	1	5	24	**32**	15	2	79	41
Moderate (51–100)	7	17	**46**	43	38	19	170	27
Unhealthy for Sensitive Groups (101–150)	8	23	17	40	**50**	20	158	32
Unhealthy (151–200)	8	16	11	21	**36**	14	106	34
Very Unhealthy (201–300)	5	4	9	17	**25**	5	65	38
Hazardous (>300)	0	3	3	7	**18**	6	37	49
total	29	68	110	160	**182**	66	615	30

In Tables 2 and 3, the days of slightly-absorbing types have the largest percentage when the AQI is greater than 150 (Unhealthy (151–200), Very Unhealthy (201–300) and Hazardous (>300)), which increased from 31% to 48% in BJ and 34% to 49% in XH. It is nearly twice as much as the other aerosol types. Particularly, the average proportion rises up to 49% when the AQI is greater than 300 (hazardous) both in BJ and XH. With increasing AQI, the proportion of days in the different AQI class with slightly-absorbing aerosols increased in BJ and XH (Tables 2 and 3). In contrast, the proportion of days in the different AQI class with mixed aerosols decreased with the increasing of the AQI in BJ (Table 2). The proportion of days in the different AQI class with highly-absorbing aerosols also decreased with increasing of the AQI in XH (Table 3). Overall, the occurred days of slightly-absorbing types remain the highest percentage throughout the polluted period (AQI > 150), which is up to 49%.

3.3.2. The Relationship between Aerosol Types and AQI

As shown in Tables 2 and 3, the incidence of each aerosol type has been obtained for the six air pollution levels, respectively. During these three years, the air quality of Beijing usually remains in the moderate and unhealthy for sensitive group levels, or even unhealthy levels, with AQI ranging from 50 to 200. In order to discuss the correlation between aerosol types and AQI, this study used the percentage of the days of different aerosol types at specific air quality levels in the three years at BJ and XH stations. Simultaneously, a correlation relationship between aerosol types and air quality was established (Figure 10). Figure 10 shows that there was an apparent relationship between aerosol type and AQI. The Pearson correlation statistics method was conducted by IBM SPSS statistics 20 [69]. The linear correlation coefficients were calculated to quantitatively examine the correlation between AQI and aerosol types. The symbols are the percentage of aerosol types at different AQI levels. There were significant differences ($p < 0.05$) between AQI and slight-absorbing (both in BJ and XH), mixed (in BJ), and highly-absorbing (in XH). This indicates that these aerosol types are closely related to AQI.

The results show that there is an excellent correlation between the slightly-absorbing aerosol types and AQI with a linear correlation coefficient of 0.76 and 0.97 in BJ and XH sites, respectively. The high correlation (0.97) between AQI and slightly-absorbing types possibly indicates that the primary air pollution source are the fine particles of vehicle emissions and industrial emissions, since the massive black carbon particles and inorganic salts may be the major components of the slightly-absorbing types [70,71]. Meanwhile, the highest linear correlation coefficient (0.83) of the mixed types was found at the BJ station, and the high linear correlation coefficient (0.73) of the highly-absorbing types was found at the XH station. Moreover, the slope is positive for slightly-absorbing aerosols but negative for the mixed aerosols. This indicates that the proportion of days in the slight-absorbing class is increased with increasing AQI. In contrast, the proportion of days in the mixed class in BJ and the proportion of days in the strong-absorbing class in XH are decreased with increasing AQI. Although the primary aerosol types are similar at BJ and XH stations, the other secondary aerosol types are different because of the regional environment. Therefore, the relationship between AQI and aerosol types also confirms that aerosol types may act as useful indicators of air quality.

In a previous study, the air pollution distribution had notable regional features in Beijing, where heavy pollution is mainly concentrated in the urban region [68]. However, in recent years, the primary atmospheric pollutant in suburban regions is $PM_{2.5}$, such as in Fangshan, Daxing, and Tongzhou. The daily maximum $PM_{2.5}$ concentration frequently exceeds 250 $\mu g\ m^{-3}$, and the AQI is up to 300, which indicates that the pollution of suburban regions has become more and more serious from 2013 to 2015. Since the start of the 21st century, the Chinese government has implemented major measures to improve air quality in Beijing. For instance, in order to directly reduce air pollution, Beijing has effectively controlled resource-based industries and vigorously expanded high-tech industries. Meanwhile, the traffic and industrial emissions have been significantly reduced by strict standards. However, a large number of factories' emissions have exerted considerable influence on air quality in suburban regions. Obviously, the air quality of suburban regions is a potential risk. Simultaneously,

meteorology can play a huge role, e.g., by bringing pollutants through long-range transport and improving photochemical processing. The wind and air pressure can bring more energy to complete the atmospheric turbulence, which could create advantageous conditions for pollutant dispersion and secondary aerosol generation. Moreover, the fine particles could increase in the case of temperature and humidity. The strong linear correlation between slightly-absorbing aerosol types and AQI has shown that the contribution of slightly-absorbing aerosols was likely more important than other aerosol types in the hazardous period. Thus, Beijing must continue to persevere with respect to the control of air pollution. In the future, the synergetic development of regions is the best way to drastically improve the regional air quality in densely-populated areas.

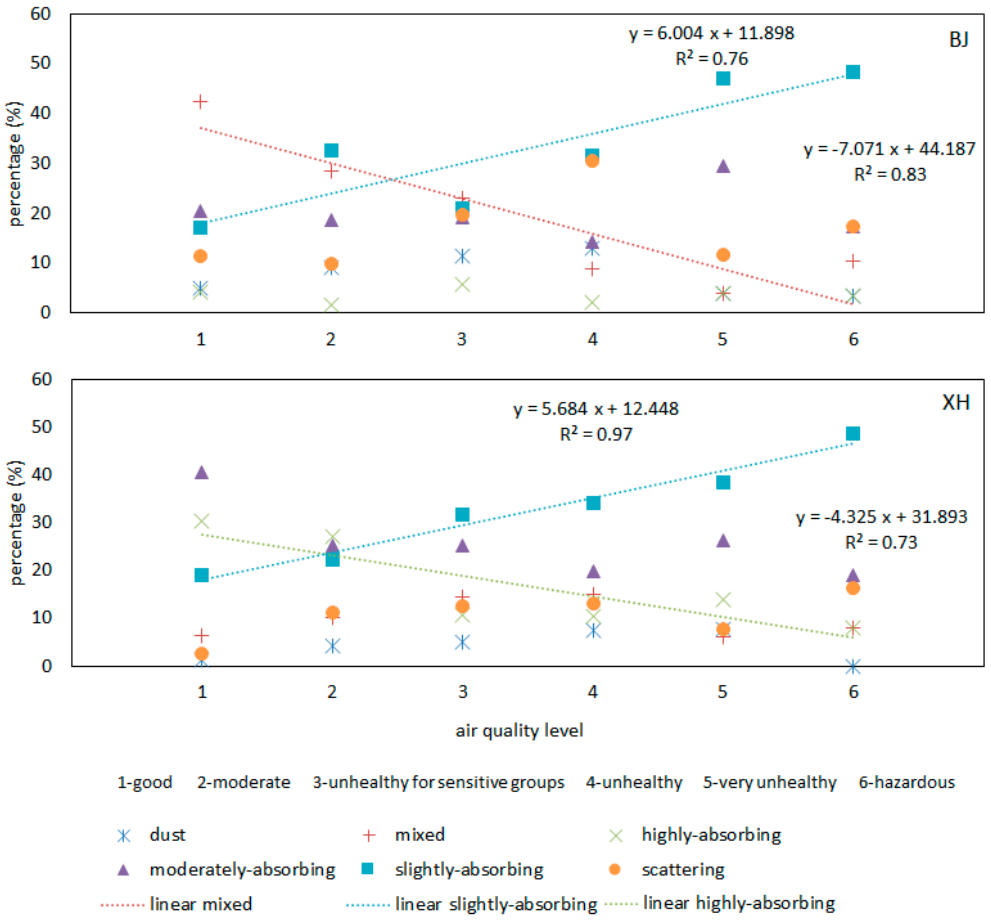

Figure 10. Linear regression of the air quality index (AQI) and the proportion of aerosol types at BJ and XH stations (2013–2015).

4. Conclusions

This study analyzed the characteristic annual and seasonal variations of aerosol types from AERONET observations between 2004 and 2015 via the comparison of two stations (BJ and XH). We discussed the relationship between the various aerosol types (dust, mixed, highly-absorbing, moderately-absorbing, slightly-absorbing and scattering) and the different AQI levels (good, moderate, unhealthy for sensitive groups, unhealthy, very unhealthy and hazardous).

The results found that the dominant aerosol of seasonal variations is similar in BJ and XH. Dust is significant in spring. The slightly-absorbing aerosols remain the highest throughout all of the seasons in both stations, especially in summer. The moderately-absorbing and highly-absorbing aerosols are significant in autumn. The mixed and highly-absorbing aerosols are dominant in winter, but the percentage of mixed aerosols in BJ was nearly double that in XH. It is illustrated that season has

a very important influence on the variation of aerosol types. From the view of the last 12 years, the slightly-absorbing aerosols remain the main aerosol types in BJ and XH stations. They are mainly caused by vehicle exhaust, industry emissions, aggravation of the incomplete burning of coal, and other factors. In summary, the aerosol types of urban sites are similar to those in suburban sites in the long-term (2004–2015). In the period of 2013–2015, the slightly-absorbing aerosols remain the highest percentage throughout the polluted period. The average proportion of days in the hazardous class with slightly-absorbing aerosols was 49%. A correlation relationship between aerosol types and air quality was established, and the results show that there is an excellent correlation between the slightly-absorbing aerosols and AQI with linear correlation coefficients of 0.76 and 0.97 in BJ and XH stations, respectively. Hence, the changes of dominant aerosol types are generally a factor in the changes in air quality over both urban and suburban regions.

Unfortunately, there are practical limitations in analyzing the characteristics of aerosol types in Beijing (including urban and suburban regions) because three years of air quality data are too short to represent the tendencies in the long-term. In future work, other methods are needed to supplement the air quality data. Although there is a strong correlation between AQI and slightly-absorbing aerosols, other meteorological factors need to be considered to estimate the air quality in the future. Additionally, the data of aerosol optical properties were collected from just two stations. Therefore, additional AERONET stations (such as Beijing-CAMS and Beijing-RADI) operating over long periods would be desirable to support studies of the regional air quality.

Acknowledgments: This research was sponsored by the Research and application of regional air quality comprehensive detection based on new generation satellite remote sensing, ground monitoring and analysis model (Z161100001116013). The authors thank the Beijing Municipal Environmental Monitoring Center for the air quantity data, and NASA for support of the BJ and XH AERONET stations.

Author Contributions: Ou Yang preformed and prepared the paper. Zhao Wenhui, Wang Junqian, Zhao Wenji and Zhang Bo provided advice and suggestions.

Conflicts of Interest: The authors declare no conflict of interest.

References

1. Mielonen, T.; Arola, A.; Komppula, M.; Kukkonen, J.; Koskinen, J.; de Leeuw, G.; Lehtinen, K.E.J. Comparison of caliop level 2 aerosol subtypes to aerosol types derived from aeronet inversion data. *Geophys. Res. Lett.* **2009**, *36*, 252–260. [CrossRef]
2. Taylor, K.E.; Penner, J.E. Response of the climate system to atmospheric aerosols and greenhouse gases. *Nature* **1994**, *369*, 734–737. [CrossRef]
3. Ramanathan, V.; Carmichael, G. Global and regional climate changes due to black carbon. *Nat. Geosci.* **2008**, *36*, 335–358. [CrossRef]
4. Streets, D.G.; Yu, C.; Wu, Y.; Chin, M.; Zhao, Z.; Hayasaka, T.; Shi, G. Aerosol trends over China, 1980–2000. *Atmos. Res.* **2008**, *88*, 174–182. [CrossRef]
5. Tie, X.; Wu, D.; Brasseur, G. Lung cancer mortality and exposure to atmospheric aerosol particles in Guangzhou, China. *Atmos. Environ.* **2009**, *43*, 2375–2377. [CrossRef]
6. Pathak, B.; Bhuyan, P.K.; Gogoi, M.; Bhuyan, K. Seasonal heterogeneity in aerosol types over Dibrugarh-north-eastern India. *Atmos. Environ.* **2012**, *47*, 307–315. [CrossRef]
7. Bibi, H.; Alam, K.; Bibi, S. In-depth discrimination of aerosol types using multiple clustering techniques over four locations in Indo-Gangetic plains. *Atmos. Res.* **2016**, *181*, 106–114. [CrossRef]
8. Dubovik, O.; Holben, B.; Eck, T.F.; Smirnov, A.; Kaufman, Y.J.; King, M.D.; Tanré, D.; Slutsker, I. Variability of absorption and optical properties of key aerosol types observed in worldwide locations. *J. Atmos. Sci.* **2002**, *59*, 590–608. [CrossRef]
9. Lee, J.; Kim, J.; Song, C.H.; Kim, S.B.; Chun, Y.; Sohn, B.J.; Holben, B.N. Characteristics of aerosol types from AERONET sunphotometer measurements. *Atmos. Environ.* **2010**, *44*, 3110–3117. [CrossRef]
10. Giles, D.M.; Holben, B.N.; Eck, T.F.; Sinyuk, A.; Smirnov, A.; Slutsker, I.; Dickerson, R.; Thompson, A.; Schafer, J. An analysis of aeronet aerosol absorption properties and classifications representative of aerosol source regions. *J. Geophys. Res. Atmos.* **2012**, *117*, 127–135. [CrossRef]

11. Andreae, M.O.; Rosenfeld, D. Aerosol–cloud–precipitation interactions. Part 1. The nature and sources of cloud-active aerosols. *Earth Sci. Rev.* **2008**, *89*, 13–41. [CrossRef]
12. Yi, B. Aerosol-cloud-precipitation relationships from satellite observations and global climate model simulations. *J. Appl. Remote Sens.* **2012**, *6*. [CrossRef]
13. Dubovik, O.; Herman, M.; Holdak, A.; Lapyonok, T.; Tanré, D.; Deuzé, J.L.; Ducos, F.; Sinyuk, A.; Lopatin, A. Statistically optimized inversion algorithm for enhanced retrieval of aerosol properties from spectral multi-angle polarimetric satellite observations. *Atmos. Meas. Tech. Discuss.* **2010**, *3*, 4967–5077. [CrossRef]
14. Yoon, J.; Pozzer, A.; Chang, D.Y.; Lelieveld, J.; Kim, J.; Kim, M.; Lee, Y.G.; Koo, J.H.; Lee, J.; Moon, K.J. Trend estimates of aeronet-observed and model-simulated AOTs between 1993 and 2013. *Atmos. Environ.* **2016**, *125*, 33–47. [CrossRef]
15. Levy, R.C.; Remer, L.A.; Mattoo, S.; Vermote, E.F.; Kaufman, Y.J. Second-generation operational algorithm: Retrieval of aerosol properties over land from inversion of moderate resolution imaging spectroradiometer spectral reflectance. *J. Geophys. Res. Atmos.* **2007**, *112*, 319–321. [CrossRef]
16. Huebert, B.J.; Bates, T.; Russell, P.B.; Shi, G.; Kim, Y.J.; Kawamura, K.; Carmichael, G.; Nakajima, T. An overview of ACE-Asia: Strategies for quantifying the relationships between Asian aerosols and their climatic impacts. *J. Geophys. Res.* **2003**, *108*. [CrossRef]
17. Tang, G.; Zhao, P.; Wang, Y.; Gao, W.; Cheng, M.; Xin, J.; Li, X.; Wang, Y. Mortality and air pollution in Beijing: The long-term relationship. *Atmos. Environ.* **2017**, *150*, 238–243. [CrossRef]
18. Wang, L.; Liu, Z.; Sun, Y.; Ji, D.; Wang, Y. Long-range transport and regional sources of $PM_{2.5}$ in Beijing based on long-term observations from 2005 to 2010. *Atmos. Res.* **2015**, *157*, 37–48. [CrossRef]
19. Zhang, R.; Wang, G.; Guo, S.; Zamora, M.L.; Ying, Q.; Lin, Y.; Wang, W.; Hu, M.; Wang, Y. Formation of urban fine particulate matter. *Chem. Rev.* **2015**, *115*, 3803–3855. [CrossRef] [PubMed]
20. Liu, Z.; Wang, Y.; Hu, B.; Ji, D.; Zhang, J.; Wu, F.; Wan, X.; Wang, Y. Source appointment of fine particle number and volume concentration during severe haze pollution in Beijing in January 2013. *Environ. Sci. Pollut. Res.* **2016**, *23*, 6845–6860. [CrossRef] [PubMed]
21. Peng, J.; Hu, M.; Guo, S.; Du, Z.; Zheng, J.; Shang, D.; Levy, Z.M.; Zeng, L.; Shao, M.; Wu, Y.S. Markedly enhanced absorption and direct radiative forcing of black carbon under polluted urban environments. *Proc. Natl. Acad. Sci. USA* **2016**, *113*, 4266–4271. [CrossRef] [PubMed]
22. Li, Z.; Xia, X.; Cribb, M.; Mi, W.; Holben, B.; Wang, P.; Chen, H.; Tsay, S.C.; Eck, T.F.; Zhao, F. Aerosol optical properties and their radiative effects in northern China. *J. Geophys. Res. Atmos.* **2007**, *112*, 321–341. [CrossRef]
23. Guo, J.P.; Zhang, X.Y.; Wu, Y.R.; Zhaxi, Y.; Che, H.Z.; Ba, L.; Wang, W.; Li, X.W. Spatio-temporal variation trends of satellite-based aerosol optical depth in China during 1980–2008. *Atmos. Environ.* **2011**, *45*, 6802–6811. [CrossRef]
24. Guo, J.; Niu, T.; Wang, F.; Deng, M.; Wang, Y. Integration of multi-source measurements to monitor sand-dust storms over north China: A case study. *Acta Meteorol. Sin.* **2013**, *27*, 566–576. [CrossRef]
25. San Martini, F.M.; Hasenkopf, C.A.; Roberts, D.C. Statistical analysis of $PM_{2.5}$ observations from diplomatic facilities in China. *Atmos. Environ.* **2015**, *110*, 174–185. [CrossRef]
26. Huang, R.J.; Zhang, Y.; Bozzetti, C.; Ho, K.F.; Cao, J.J.; Han, Y.; Daellenbach, K.R.; Slowik, J.G.; Platt, S.M.; Canonaco, F. High secondary aerosol contribution to particulate pollution during haze events in China. *Nature* **2014**, *514*, 218–222. [CrossRef] [PubMed]
27. Guo, S.; Hu, M.; Zamora, M.L.; Peng, J.; Shang, D.; Zheng, J.; Du, Z.; Wu, Z.; Shao, M.; Zeng, L. Elucidating severe urban haze formation in China. *Proc. Natl. Acad. Sci. USA* **2014**, *111*, 17373–17378. [CrossRef] [PubMed]
28. Li, Z.; Gu, X.; Wang, L.; Li, D.; Xie, Y.; Li, K.; Dubovik, O.; Schuster, G.; Goloub, P.; Zhang, Y.; et al. Aerosol physical and chemical properties retrieved from ground-based remote sensing measurements during heavy haze days in Beijing winter. *Atmos. Chem. Phys.* **2013**, *13*, 10171–10183. [CrossRef]
29. Zhang, Z.; Zhang, X.; Gong, D.; Quan, W.; Zhao, X.; Ma, Z.; Kim, S.J. Evolution of surface O_3 and $PM_{2.5}$ concentrations and their relationships with meteorological conditions over the last decade in Beijing. *Atmos. Environ.* **2015**, *108*, 67–75. [CrossRef]
30. Eck, T.F.; Holben, B.N.; Dubovik, O.; Smirnov, A.; Goloub, P.; Chen, H.B.; Chatenet, B.; Gomes, L.; Zhang, X.Y.; Tsay, S.C. Columnar aerosol optical properties at AERONET sites in central eastern Asia and aerosol transport to the tropical mid-pacific. *J. Geophys. Res. Atmos.* **2005**, *110*, 887–908. [CrossRef]

31. Kim, S.W.; Yoon, S.C.; Kim, J.; Kim, S.Y. Seasonal and monthly variations of columnar aerosol optical properties over east Asia determined from multi-year MODIS, LIDAR, and AERONET sun/sky radiometer measurements. *Atmos. Environ.* **2007**, *41*, 1634–1651. [CrossRef]
32. Wang, L.; Xin, J.; Li, X.; Wang, Y. The variability of biomass burning and its influence on regional aerosol properties during the wheat harvest season in north China. *Atmos. Res.* **2015**, *157*, 153–163. [CrossRef]
33. He, K.; Yang, F.; Ma, Y.; Zhang, Q.; Yao, X.; Chan, C.K.; Cadle, S.; Chan, T.; Mulawa, P. The characteristics of $PM_{2.5}$ in Beijing, China. *Atmos. Environ.* **2001**, *35*, 4959–4970. [CrossRef]
34. Zhu, L.; Huang, X.; Shi, H.; Cai, X.; Song, Y. Transport pathways and potential sources of PM_{10} in Beijing. *Atmos. Environ.* **2011**, *45*, 594–604. [CrossRef]
35. Liu, X.G.; Li, J.; Qu, Y.; Han, T.; Hou, L.; Gu, J.; Chen, C.; Yang, Y.; Liu, X.; Yang, T. Formation and evolution mechanism of regional haze: A case study in the megacity Beijing, China. *Atmos. Chem. Phys.* **2013**, *13*, 4501–4514. [CrossRef]
36. Quan, J.; Gao, Y.; Zhang, Q.; Tie, X.; Cao, J.; Han, S.; Meng, J.; Chen, P.; Zhao, D. Evolution of planetary boundary layer under different weather conditions, and its impact on aerosol concentrations. *Particuology* **2013**, *11*, 34–40. [CrossRef]
37. Zhang, R.; Jing, J.; Tao, J.; Hsu, S.C. Chemical characterization and source apportionment of $PM_{2.5}$ in Beijing: Seasonal perspective. *Atmos. Chem. Phys.* **2013**, *13*, 7053–7074. [CrossRef]
38. Li, W.J.; Shao, L.Y.; Buseck, P.R. Haze types in Beijing and the influence of agricultural biomass burning. *Atmos. Chem. Phys.* **2010**, *10*, 8119–8130. [CrossRef]
39. Yan, P.; Pan, X.; Tang, J.; Zhou, X.; Zhang, R.; Zeng, L. Hygroscopic growth of aerosol scattering coefficient: A comparative analysis between urban and suburban sites at winter in Beijing. *Particuology* **2009**, *7*, 52–60. [CrossRef]
40. Duan, F.; Liu, X.; Yu, T.; Cachier, H. Identification and estimate of biomass burning contribution to the urban aerosol organic carbon concentrations in Beijing. *Atmos. Environ.* **2004**, *38*, 1275–1282. [CrossRef]
41. Zhao, X.J.; Zhao, P.S.; Xu, J.; Meng, W.; Pu, W.W.; Dong, F.; He, D.; Shi, Q.F. Analysis of a winter regional haze event and its formation mechanism in the north China plain. *Atmos. Chem. Phys.* **2013**, *13*, 5685–5696. [CrossRef]
42. Tang, G.; Zhang, J.; Zhu, X.; Song, T.; Münkel, C.; Hu, B.; Schäfer, K.; Liu, Z.; Zhang, J.; Wang, L. Mixing layer height and its implications for air pollution over Beijing, China. *Atmos. Chem. Phys. Discuss.* **2016**, *16*, 2459–2475. [CrossRef]
43. Li, J.; Wang, G.; Ren, Y.; Wang, J.; Wu, C.; Han, Y.; Zhang, L.; Cheng, C.; Meng, J. Identification of chemical compositions and sources of atmospheric aerosols in Xi'an, inland China during two types of haze events. *Sci. Total Environ.* **2016**, *566–567*, 230–237. [CrossRef] [PubMed]
44. Eck, T.F.; Holben, B.N.; Sinyuk, A.; Pinker, R.T.; Goloub, P.; Chen, H.; Chatenet, B.; Li, Z.; Singh, R.P.; Tripathi, S.N.; et al. Climatological aspects of the optical properties of fine/coarse mode aerosol mixtures. *J. Geophys. Res.* **2010**, *115*. [CrossRef]
45. Wang, Y.; Xin, J.; Li, Z.; Wang, S.; Wang, P.; Hao, W.M.; Nordgren, B.L.; Chen, H.; Wang, L.; Sun, Y. Seasonal variations in aerosol optical properties over China. *J. Geophys. Res.* **2011**, *116*. [CrossRef]
46. Yu, X.; Lu, R.; Kumar, K.R.; Ma, J.; Zhang, Q.; Jiang, Y.; Kang, N.; Yang, S.; Wang, J.; Li, M. Dust aerosol properties and radiative forcing observed in spring during 2001–2014 over urban Beijing, China. *Environ. Sci. Pollut. Res. Int.* **2016**, *23*, 15432–15442. [CrossRef] [PubMed]
47. Wang, Y.; Zhuang, G.; Sun, Y.; An, Z. The variation of characteristics and formation mechanisms of aerosols in dust, haze, and clear days in Beijing. *Atmos. Environ.* **2006**, *40*, 6579–6591. [CrossRef]
48. Li, S.; Xiang-Ao, X.; Pu-Cai, W.; Hong-Bin, C.; Goloub, P.; Wen-Xing, Z. Identification of aerosol types and their optical properties in the north China plain based on long-term AERONET data. *Atmos. Ocean. Sci. Lett.* **2013**, *6*, 216–222. [CrossRef]
49. Chen, W.; Tang, H.; Zhao, H.; Yan, L. Analysis of aerosol properties in Beijing based on ground-based sun photometer and air quality monitoring observations from 2005 to 2014. *Remote Sens.* **2016**, *8*. [CrossRef]
50. Ou, Y.; Chen, F.; Zhao, W.; Yan, X.; Zhang, Q. Landsat 8-based inversion methods for aerosol optical depths in the Beijing area. *Atmos. Pollut. Res.* **2017**, *8*, 267–274. [CrossRef]
51. Kuang, W.; Du, G. Analyzing urban population spatial distribution in Beijing proper. *J. Geo-Inf. Sci.* **2011**, *13*, 506–512. [CrossRef]

52. Dubovik, O.; Smirnov, A.; Holben, B.N.; King, M.D.; Kaufman, Y.J.; Eck, T.F.; Slutsker, I. Accuracy assessments of aerosol optical properties retrieved from aerosol robotic network (AERONET) sun and sky radiance measurements. *J. Geophys. Res. Atmos.* **2000**, *105*, 9791–9806. [CrossRef]
53. Sun, L.; Wei, J.; Bilal, M.; Tian, X.; Jia, C.; Guo, Y.; Mi, X. Aerosol optical depth retrieval over bright areas using Landsat 8 OLI images. *Remote Sens.* **2015**, *8*. [CrossRef]
54. Kim, H.S.; Chung, Y.S.; Lee, S.G. Characteristics of aerosol types during large-scale transport of air pollution over the yellow sea region and at Changwon, Korea, in 2008. *Environ. Monit. Assess.* **2012**, *184*, 1973–1984. [CrossRef] [PubMed]
55. Kaskaoutis, D.G.; Kosmopoulos, P.; Kambezidis, H.D.; Nastos, P.T. Aerosol climatology and discrimination of different types over Athens, Greece, based on MODIS data. *Atmos. Environ.* **2007**, *41*, 7315–7329. [CrossRef]
56. Kaskaoutis, D.G.; Kambezidis, H.D.; Hatzianastassiou, N.; Kosmopoulos, P.G. Aerosol climatology: Dependence of the angstrom exponent on wavelength over four AERONET sites. *Atmos. Environ.* **2007**, *41*, 7315–7329. [CrossRef]
57. Kumar, K.R.; Sivakumar, V.; Reddy, R.R.; Gopal, K.R.; Adesina, A.J. Identification and classification of different aerosol types over a subtropical rural site in Mpumalanga, South Africa: Seasonal variations as retrieved from the AERONET Sunphotometer. *Aerosol Air Qual. Res.* **2014**, *14*, 108–123. [CrossRef]
58. Kumar, K.R.; Yin, Y.; Sivakumar, V.; Kang, N.; Yu, X.; Diao, Y.; Adesina, A.J.; Reddy, R.R. Aerosol climatology and discrimination of aerosol types retrieved from MODIS, MISR and OMI over Durban (29.88°S, 31.02°E), South Africa. *Atmos. Environ.* **2015**, *117*, 9–18. [CrossRef]
59. Xu, W.; Chen, H.; Li, D.; Zhao, F.; Yang, Y. A case study of aerosol characteristics during a haze episode over Beijing. *Procedia Environ. Sci.* **2013**, *18*, 404–411. [CrossRef]
60. Van Donkelaar, A.; Martin, R.V.; Brauer, M.; Kahn, R.; Levy, R.; Verduzco, C.; Villeneuve, P.J. Global estimates of ambient fine particulate matter concentrations from satellite-based aerosol optical depth: Development and application. *Environ. Health Perspect.* **2010**, *118*, 847–855. [CrossRef] [PubMed]
61. Levy, R.C.; Remer, L.A.; Dubovik, O. Global aerosol optical properties and application to moderate resolution imaging spectroradiometer aerosol retrieval over land. *J. Geophys. Res. Atmos.* **2007**, *112*, 3710–3711. [CrossRef]
62. Smirnov, A.; Holben, B.N.; Eck, T.F.; Dubovik, O.; Slutsker, I. Cloud-screening and quality control algorithms for the AERONET database. *Remote Sens. Environ.* **2000**, *73*, 337–349. [CrossRef]
63. Chen, H.; Gu, X.; Cheng, T.; Yu, T.; Li, Z. Characteristics of aerosol types over China. *J. Remote Sens.* **2013**, *17*, 1559–1571.
64. Moosmüller, H.; Chakrabarty, R.K.; Arnott, W.P. Aerosol light absorption and its measurement: A review. *J. Quant. Spectrosc. Radiat. Transf.* **2009**, *110*, 844–878. [CrossRef]
65. Nessler, R.; Weingartner, E.; Baltensperger, U. Effect of humidity on aerosol light absorption and its implications for extinction and the single scattering albedo illustrated for a site in the lower free troposphere. *J. Aerosol Sci.* **2005**, *36*, 958–972. [CrossRef]
66. Chen, Y.; Schleicher, N.; Fricker, M.; Cen, K.; Liu, X.-l.; Kaminski, U.; Yu, Y.; Wu, X.-f.; Norra, S. Long-term variation of black carbon and $PM_{2.5}$ in Beijing, China with respect to meteorological conditions and governmental measures. *Environ. Pollut.* **2016**, *212*, 269–278. [CrossRef] [PubMed]
67. Meng, J.; Liu, J.; Guo, S.; Li, J.; Li, Z.; Tao, S. Trend and driving forces of Beijing's black carbon emissions from sectoral perspectives. *J. Clean. Prod.* **2016**, *112*, 1272–1281. [CrossRef]
68. Cheng, W.-L.; Chen, Y.-S.; Zhang, J.; Lyons, T.; Pai, J.-L.; Chang, S.-H. Comparison of the revised air quality index with the psi and aqi indices. *Sci. Total Environ.* **2007**, *382*, 191–198. [CrossRef] [PubMed]
69. Field, A. *Discovering Statistics Using IBM SPSS Statistics*, 4th ed.; Sage Publications Ltd.: Los Angeles, CA, USA, 2013.
70. Xia, X.A.; Chen, H.B.; Wang, P.C.; Zong, X.M.; Qiu, J.H.; Gouloub, P. Aerosol properties and their spatial and temporal variations over north China in spring 2001. *Tellus Ser. B Chem. Phys. Meteorol.* **2005**, *57*, 28–39.
71. Cairncross, E.K.; John, J.; Zunckel, M. A novel air pollution index based on the relative risk of daily mortality associated with short-term exposure to common air pollutants. *Atmos. Environ.* **2007**, *41*, 8442–8454. [CrossRef]